J Solid State Electrochem (2007) 11:1279–1286
DOI 10.1007/s10008-007-0287-3

ORIGINAL PAPER

Composite films of polyaniline and molybdenum oxide formed by electrocodeposition in aqueous media

Xiao-Xia Liu · Li-Jun Bian · Lu Zhang · Li-Jun Zhang

Received: 10 October 2006 / Revised: 6 December 2006 / Accepted: 6 February 2007 / Published online: 24 February 2007

Abstract Composite films of polyaniline (PANI) and molybdenum oxide (MoO_x) were afforded through a convenient route of electrocodeposition from aniline and $(NH_4)_6Mo_7O_{24}$. The composite films showed characteristic redox behaviors of PANI and MoO_x, respectively, on the cyclic voltammograms. Chlorate and bromate were catalytically electroreduced with an enlarged current on the composite film at a potential ca. 0.2 V more positive than that on MoO_x. The potential window for the composite film to display pseudocapacitive properties in 1.0 mol·dm^{-3} $NaNO_3$ was −0.6 ~ 0.6 V vs SCE. The cathodic potential limit shifted at least 0.4 V negatively from that of polyaniline (PANI)-based materials reported so far. The specific capacitance was 363.6 F·g^{-1} when the composite film was charged–discharged at 1.5 mA·cm^{-2}, about two times of that of the similarly prepared PANI. The composite film was characterized by Fourier transform infrared (FTIR) spectroscopy, X-ray diffraction (XRD), and X-ray photoelectron spectroscopy (XPS). Molybdenum existed in a mixed state of +5 and +6 in the composite film based on XRD and XPS investigations.

Keywords Polyaniline · Molybdenum oxide · Electrocodeposition · Electrocatalysis · Pseudocapacitive properties

Introduction

Composite materials consisting of conducting polymers and inorganic particles have attracted considerable attention, as they can combine the advantages of both components and may offer special properties through the reinforcement or modification of each other [1]. Polyaniline (PANI) has been widely studied, as it has promising applications in a variety of technologic fields, such as electrochemical supercapacitors, batteries, sensors, and corrosion inhibitors, ect. [2]. The properties of PANI can be modified by incorporation of other functional materials including inorganic particles [3, 4]. On the other hand, PANI can provide a conducting network for inorganic components and modify the latter [5]. MoO_x has recently received much attention owing to its interesting electrochemical, electrochromic, and electrocatalytic properties [6–12]. It can also modify the properties of other materials through composition [13, 14]. The composite film of PANI and MoO_x is, thus, expected to exhibit synergistic effects.

The composites of PANI and MoO_3 were reported to be obtained through concomitant ion-exchange polymerization or ex situ intercalation. The $(PANI)_xMoO_3$ nanocomposites displayed modified properties for lithium battery or volatile organic compounds sensors [15, 16]. Electrocodeposition is an effective way to make composite films with a large variety of tunable parameters and so the advantage of convenient film control [17]. However, the traditional method for the electrodeposition of PANI is conducted through oxidative electropolymerization of aniline in low pH aqueous solutions, while metal oxides are likely to electrodeposit cathodically and usually in high pH media. Reports about the electrodeposition of composites based on PANI and metal oxide are very limited [5].

MoO_x was reported to electrodeposit from oxometalate anions when the potential domain was extended negatively to ca. −0.7 V vs SCE in slightly acidic to neutral solutions [6, 10, 11, 18]. Recently, we studied the electropolymerization of aniline in aqueous solutions of pH 2 to 12 and

X.-X. Liu (✉) · L.-J. Bian · L. Zhang · L.-J. Zhang
Department of Chemistry, Northeastern University,
Shenyang 110004, People's Republic of China
e-mail: xxliu@mail.neu.edu.cn

successfully obtained electroactive PANI in the whole pH range studied [19]. Therefore, electrocodeposition of PANI and MoO_x can be tried through large-scale potential cycling in slightly acidic to neutral solutions. In this paper, syntheses of PANI–MoO_x composite films are performed electrochemically for the first time by cyclic voltammetry in aqueous solutions. The electrocatalytic activities of the composite film are observed through the reduction of oxoanions, such as chlorate and bromate. Pseudocapacitive properties of the composite film in 1 mol·dm^{-3} $NaNO_3$ are studied through cyclic voltammetry and constant current charge–discharge experiments. Characterizations of PANI–MoO_x are conducted by Fourier transform infrared (FTIR) spectroscopy, X-ray diffraction (XRD), and X-ray photoelectron spectroscopy (XPS).

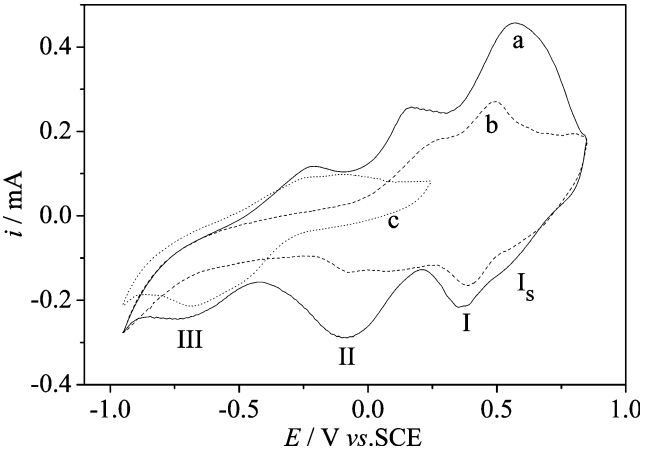

Fig. 1 Cyclic voltammograms of similarly prepared PANI–MoO_x C1 (**a**, *solid line*), PANI P1 (**b**, *dash line*), and MoO_x M1 (**c**, *dot line*) in 0.1 mol·dm^{-3} H_2SO_4 solution; SCE reference electrode; scan rate, v= 50 mV·s^{-1}

Materials and methods

Electrochemical experiments were performed on Princeton Applied Research model 273 potentiostat/galvanostat or electrochemical analyzer systems, CHI 660B, under ambient condition. Electrodeposition was conducted on carbon cloth electrode, or indium tin oxide (ITO) glass for XRD measurement, with platinum wire as the counter electrode. Before electrodeposition, the carbon cloth electrode was cleaned by acetone and distilled water and then, as mentioned, pre-treated by three cyclic voltammetric scans during −2.0∼2.0 V at 100 mV·s^{-1} in 2.0 mol·dm^{-3} H_2SO_4. The electrocodeposition of PANI and MoO_x was conducted in phosphate buffer solution (containing 0.1 mol·dm^{-3} KNO_3 as supporting electrolyte) by cyclic voltammetries in potential range of −0.6∼0.9 V at 50 mV·s^{-1}, using aniline (An, distilled before use) and $(NH_4)_6Mo_7O_{24}$ as precursors of the polymer and oxide, respectively. The potentials were measured and reported vs SCE. The composite films obtained in the solution of pH 1.7 containing 0.1 mol·dm^{-3} aniline and 7.5×10^{-3} mol·dm^{-3} $(NH_4)_6Mo_7O_{24}$ or 0.15 mol·dm^{-3} aniline and 7.5×10^{-3} mol·dm^{-3} $(NH_4)_6Mo_7O_{24}$ through seven consecutive cyclic scans were denoted as C1 and C2, respectively, while the composite film electrodeposited from 0.1 mol·dm^{-3} aniline and 1.5×10^{-2} mol·dm^{-3} $(NH_4)_6Mo_7O_{24}$ on pretreated carbon cloth through 30 consecutive scans was denoted as C3. The films of PANI or MoO_x electrodeposited similarly as above were denoted as P1, P2, P3, and M1, M2, M3.

The electroactivities of the films were studied through cyclic voltammetries at 50 mV·s^{-1} in 0.1 mol·dm^{-3} H_2SO_4.

Electrocatalytic experiments were conducted in 0.1 mol·dm^{-3} H_2SO_4 containing corresponding oxoanions.

The pseudocapacitive properties of the films were studied through cyclic voltammetries at 10 mV·s^{-1} and a constant current charge–discharge experiment by chronopotentiometry (CP) at 1.5 mA·cm^{-2} between −0.6 and 0.6 V in 1.0 mol·dm^{-3} $NaNO_3$. The loading of the film-coated electrode is the weight difference of the electrode (vacuum dried at room temperature) before and after electrodeposition through a microbalance with an accuracy of 0.01 mg (Sartorius BP 211D, Germany).

A spectrum one FTIR spectrophotometer was used to obtain FTIR spectra of PANI–MoO_x and PANI with KBr pellets. XRD measurement was performed with an X'Pert Pro MPD PW3040/60 X-ray diffractometer employing monochromatized Cu K_α incident radiation. XPS spectra were recorded on an Escalab Mark II electron spectrometer using Al K_α radiation (1486.6 eV).

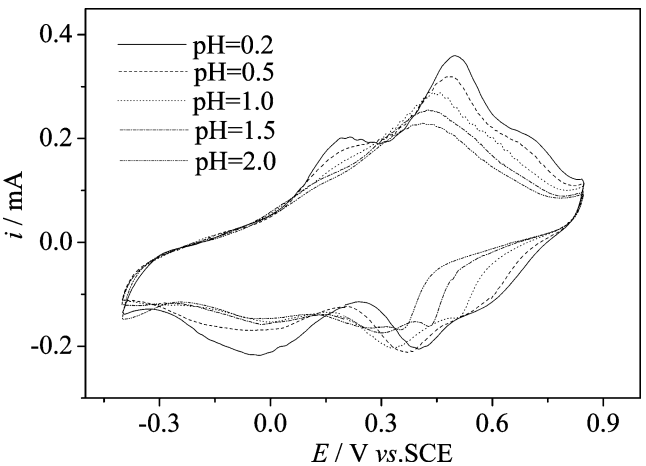

Fig. 2 Cyclic voltammograms of PANI–MoO_x C1 in solutions of different pH; SCE reference electrode; scan rate, v=50 mV·s^{-1}

Scheme 1 Exchange between the leucoemeraldine and the emeraldine states of PANI in solutions of pH 0.2 to 2

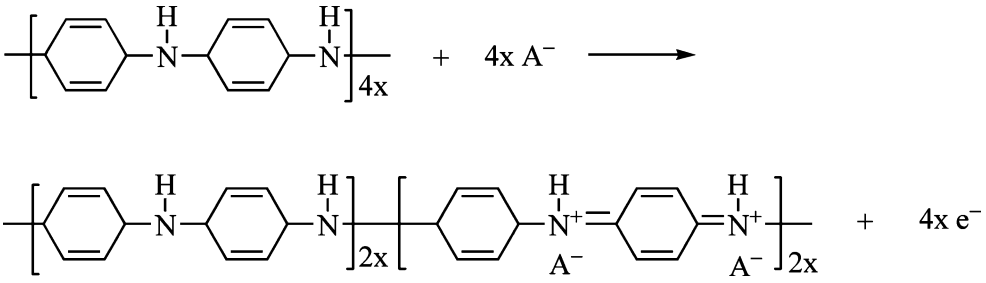

Results and discussion

Electrochemical syntheses of PANI–MoO_x

MoO_x films were reported to electrodeposit from oxometalate anions, including MoO_4^{2-} or Keggin and Dawson-type heteropolyanions through cyclic voltammetries with the cathodic potential limit of ca. −0.7 V or from $Mo_7O_{24}^{6-}$ at a constant cathodic current [6, 10–12, 18]. Electroactive PANI can be obtained electrochemically by several methods including cyclic voltammetries between ca. −0.3 and 1.0 V [20]. In this paper, the electrocodeposition of PANI and MoO_x is conducted on carbon cloth through cyclic voltammetries between −0.6 and 0.9 V.

Figure 1 is the cyclic voltammogram (CV) in monomer-free 0.1 $mol{\cdot}dm^{-3}$ H_2SO_4 of the PANI–MoO_x composite film C1 obtained in the solution of pH 1.7, containing 0.1 $mol{\cdot}dm^{-3}$ aniline and 7.5×10^{-3} $mol{\cdot}dm^{-3}$ $(NH_4)_6Mo_7O_{24}$ through seven consecutive cyclic scans (curve a), together with those of similarly prepared PANI P1 (curve b) and MoO_x M1 (curve c). The CV of the composite film C1 (curve a) shows three redox couples with shoulder peaks on the right hand of the first one. Compared to the CV of the PANI film P1 (curve b) and according to other's work [21], peaks I, II, and I_s (the shoulder peak of I) should be ascribed to the redox processes of PANI. To study the corresponding electrochemical reactions further, the film is potential scanned in H_2SO_4 solutions of pH 0.2 to 2 (Fig. 2). The potential of peak II is relatively insensitive to the changes in pH, while those of peak I and its shoulder peak I_s negatively shift as the acidity of the solution decreased. It was proposed that the extensive π conjugation in the polymer chain of the emeraldine-salt form of PANI, and hence, the high conductivity of the polymer came from the preferential protonation of the imine nitrogen, although the amine nitrogen atoms are stronger bases [21]. And, the emeraldine and the leucoemeraldine states of PANI were nearly partial and not protonated, respectively, in the pH range of our experiment, so the exchange between these two states almost did not accompany the interchange of proton between the polymer and the solution (Scheme 1) [21]. The extent of the protonation of the polymer decreases with the increasing oxidation state, so the pernigraniline state of PANI should be very little or not protonated in these solutions. Therefore, two protons per electron will accompany with the exchange between pernigraniline and the partial protonated emeraldine (Scheme 2) [21]. Figure 3 displays the change of reductive peak potentials against pH for I and I_s. From Fig. 3, the reductive peak potential of I_s shifts nearly −120 mV per pH unit in this pH range, indicating that two protons are transferred per electron. This result is in accordance with the work of A. G. MacDiarmid for redox reactions between pernigraniline and emeraldine in the similar pH range [21]. Therefore, I_s should be corresponding to the exchange between the pernigraniline and emeraldine states of PANI. The reductive potential of peak I shifts ca. −60 mV per pH unit (Fig. 3). It should be associated with the redox processes of other structures in the polymer chain.

PANI–MoO_x C1, as well as the film of MoO_x M1 made under similar conditions, shows a similar broad reductive peak at around −0.6 V on CVs in 0.1 $mol{\cdot}dm^{-3}$ H_2SO_4 solution (Fig. 1, curve a for PANI–MoO_x C1 and curve c for MoO_x M1). MoO_x film was reported to display a redox couple around −0.5 V that was ascribed to the conversion between Mo (VI) and Mo (V) [6, 11]. This peak can be similarly ascribed to this conversion.

Scheme 2 Exchange between the emeraldine and the pernigraniline states of PANI in solutions of pH 0.2 to 2

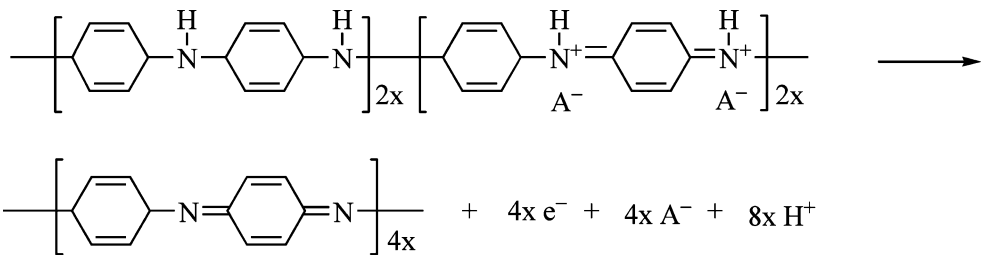

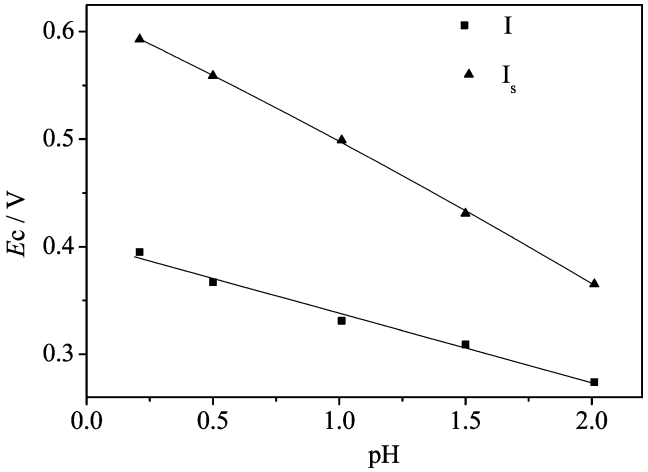

Fig. 3 Plot of reductive potentials of peak I and its shoulder (I_s) as a function of pH

Electrocatalytic reduction of oxoanions on PANI–MoO_x

It was reported that the MoO_x film exhibited catalytic activities toward the electroreduction of oxoanions in acidic aqueous media [10, 11]. To study the electrocatalytic activity of the composite film, electroreduction of oxoanions is conducted on PANI–MoO_x C2 made in the solution of 0.15 mol·dm^{-3} aniline and 7.5×10^{-3} mol·dm^{-3} $(NH_4)_6Mo_7O_{24}$ (pH 1.7). Figure 4 is the CVs in 0.1 mol·dm^{-3} H_2SO_4 containing 0.1 mol·dm^{-3} ClO_3^-. There is no evident catalytic current detected on the CVs recorded on carbon cloth and similarly prepared PANI P2 in the cyclic potential range (Fig. 4, cure a and b). A distinct current wave appears around −0.3 V for the reduction of ClO_3^- at similarly electrodeposited MoO_x M2 (Fig. 4, cure c), while the electroreduction of ClO_3^- occurs at a more positive potential (−0.09 V) on PANI–MoO_x C2 with a higher current (Fig. 4, curve d). PANI should exist in emeraldine form at this potential (see Fig. 1) and likely to be protonated in this media. Therefore, the concentration of positive-charged particles is high in PANI matrix. This will facilitate the formation of lower oxidation state molybdenum oxide (MoO_3^{x-}) and so the electroreduction of ClO_3^-. This hypothesis is supported by the formation of the hybrid material of $(PANI)_xMoO_3$ through the electrostatic interaction between the positively charged PANI and the negatively charged MoO_3^{x-} [16]. The 3D network PANI provided also facilitates the contact of the active particles with electrolyte that enhances the catalytic activities of the film. The electroreduction of BrO_3^- on the composite film displays a similar synergistic effect.

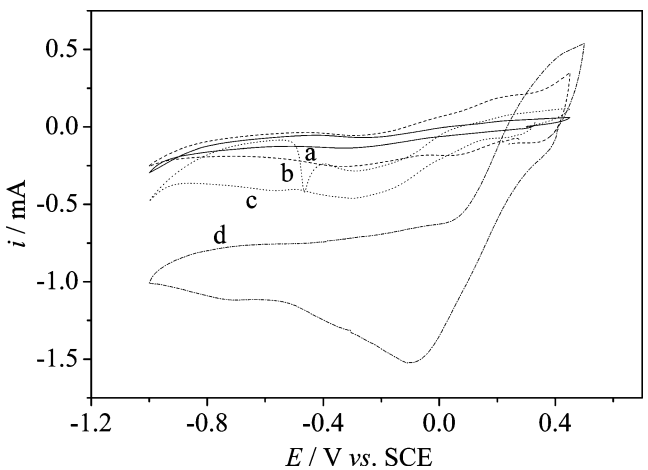

Fig. 4 Cyclic voltammograms of carbon cloth (**a**, *solid line*) and similarly prepared PANI P2 (**b**, *dash line*), MoO_x M2 (**c**, *dot line*), and PANI–MoO_x C2 (**d**, *dash–dot line*) in 0.1 mol·dm^{-3} H_2SO_4 solution containing 0.1 mol·dm^{-3} ClO_3^-; SCE reference electrode; scan rate, v=50 mV·s^{-1}

Figures 5 and 6 are the CVs on the composite film C2 in 0.1 mol·dm^{-3} H_2SO_4 containing chlorate and bromate in different concentrations. The solid lines in Figs. 5 and 6 are the voltammograms in the oxoanion-free solution. Similarly, as in Dong's work, the cathodic currents of oxoanion increase with increasing concentration of ClO_3^- or BrO_3^- [11]. The cathodic current at potential near 0 V is linear with the concentration from 15 to 100 mmol·dm^{-3} for chlorate (currents at −0.076 V) and 0.75 to 7.5 mmol·dm^{-3} for bromate (currents at 0.007 V), respectively (see insets in Figs. 5 and 6). This provides the composite film potential applications in analytical procedures for determining the oxoanions.

Pseudocapacitive properties of PANI–MoO_x

PANI is considered as a promising electrode material for supercapacitors, and its performance can be modified by

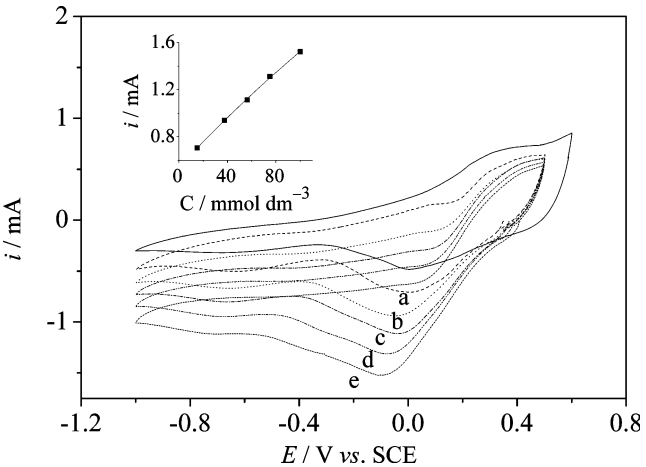

Fig. 5 Cyclic voltammograms of PANI–MoO_x C2 in 0.1 mol·dm^{-3} H_2SO_4 solution containing various concentrations of ClO_3^- together with those of C2 in ClO_3^- free solution (*solid line*); SCE reference electrode; scan rate, v=50 mV·s^{-1}. **a** *Dash line*, 15 mmol·dm^{-3} ClO_3^-; **b** *dot line*, 38 mmol·dm^{-3}ClO_3^-; **c** *dash–dot line*, 56 mmol·dm^{-3} ClO_3^-; **d** *dash–dot dot line*, 75 mmol·dm^{-3} ClO_3^-; **e** *short dash line*, 100 mmol·dm^{-3}ClO_3^-. *Inset*, plot of ClO_3^- reductive currents at −0.076 V as a function of the concentration of ClO_3^-

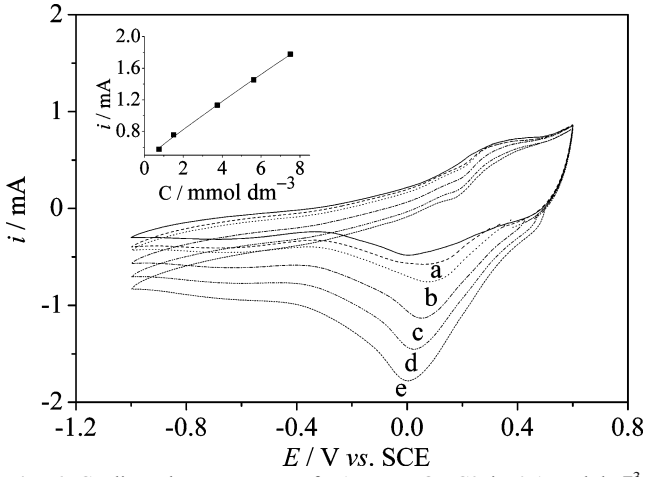

Fig. 6 Cyclic voltammograms of PANI–MoO_x C2 in 0.1 mol·dm^{-3} H_2SO_4 solution containing various concentrations of BrO_3^- together with those of C2 in BrO_3^- free solution (*solid line*); SCE reference electrode; scan rate, v=50 mV·s^{-1}. **a** *Dash line*, 0.75 mmol·dm^{-3} BrO_3^-; **b** *dot line*, 1.5 mmol·dm^{-3}BrO_3^-; **c** *dash–dot line*, 3.8 mmol·dm^{-3} BrO_3^-; **d** *dash–dot–dot line*, 5.6 mmol·dm^{-3} BrO_3^-; **e** *short dash line*, 7.5 mmol·dm^{-3} BrO_3^-. *Inset*, plot of BrO_3^- reductive currents at − 0.007 V as a function of the concentration of BrO_3^-

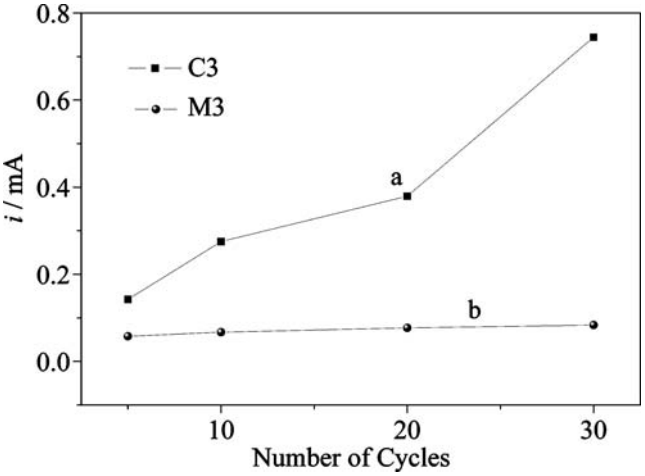

Fig. 8 Currents at −0.3 V on cyclic voltammograms in 1.0 mol·dm^{-3} $NaNO_3$ solution for films made through 5, 10, 20, and 30 cycles. **a** PANI–MoO_x C3a–d; **b** MoO_x M3a–d

composition with other functional materials [22]. To study the pseudocapacitive properties of the composite film, PANI and MoO_x are electrocodeposited on pre-treated carbon cloth by potential scans in the solution of pH 6.1 containing 0.1 mol·dm^{-3} aniline and 1.5×10^{-2} mol·dm^{-3} $(NH_4)_6Mo_7O_{24}$ to form the composite C3. Curves a, b, and c in Fig. 7 represent the voltammeric behaviors in 1.0 mol·dm^{-3} $NaNO_3$ of PANI–MoO_x C3, similarly prepared PANI P3 and MoO_x M3. The shape of the CV of PANI–MoO_x C3 (curve a) shows a roughly rectangular mirror image from −0.6 to 0.6 V, characteristic of capacitive behavior. Thus, the composite C3 displays a pseudocapacitive behavior in this potential range. To the best of our knowledge, there is no report about PANI-based material to show so negative potential limit for pseudocapacitors [22]. From Fig. 7, the capacitive properties are modified by the incorporation of MoO_x into the PANI film, especially in the negative potential range. To study the influence of MoO_x on the capacitive properties of the film, the PANI–MoO_x composite films C3a to C3d made through 5, 10, 20, and 30 potential cycles are investigated using cyclic voltammetry in 1.0 mol·dm^{-3} $NaNO_3$. The current increases as potential cycles for electrodeposition increase, especially in the potential range negative rather than 0 V. The relationship of the currents at −0.3 V on the CVs for composite films C3a to C3d with the number of cycles for electrodeposition are in Fig. 8 (curve a). Curve b displays this relationship for similarly prepared films of MoO_x M3a to M3d. The currents of the composite film C3 are larger and increase more sharply as the electrodeposition cycles increase. This

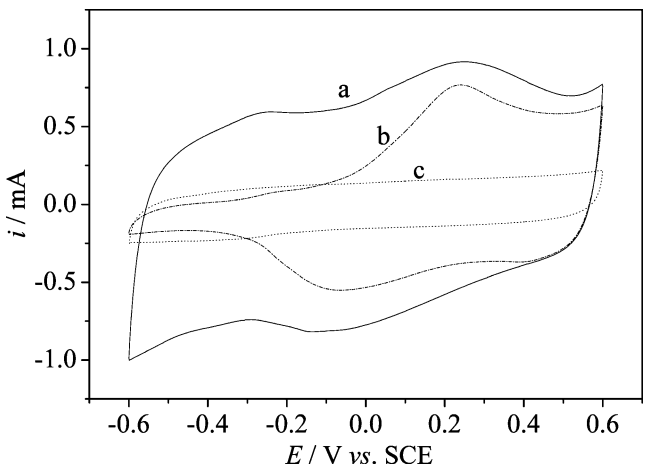

Fig. 7 Cyclic voltammograms of similarly prepared PANI–MoO_x C3 (**a**, *solid line*), PANI P3 (**b**, *dash line*), and MoO_x C3 (**c**, *dot line*) in 1.0 mol·dm^{-3} $NaNO_3$ solution; SCE reference electrode; scan rate, v= 10 mV·s^{-1}

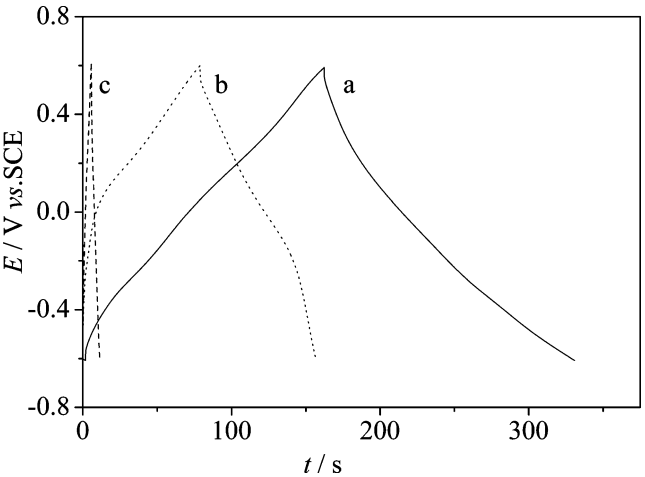

Fig. 9 Chronopotentiograms of PANI–MoO_x C3 (**a**, *solid line*) and similarly prepared PANI P3 (**b**, *dot line*), MoO_x M3 (**c**, *dash line*) in 1.0 mol·dm^{-3} $NaNO_3$ at 1.5 mA·cm^{-2}

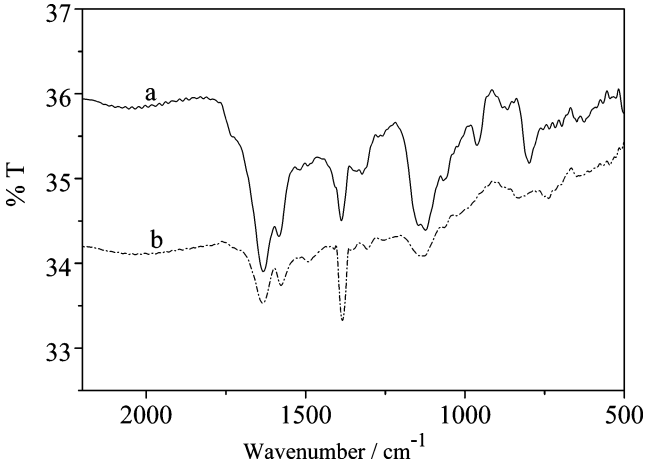

Fig. 10 FTIR spectra of similarly prepared PANI–MoO_x C3 (**a**, *solid line*) and PANI P3 (**b**, *dash–dot line*)

may be due to the 3D system of the polymer matrix that offers large effective area and facilitates the contribution of MoO_x to the pseudocapacitance of the film [23].

The charge and discharge behaviors of PANI–MoO_x C3, PANI P3, and MoO_x M3 films are examined by chronopotentiometries (CP) in 1.0 mol·dm^{-3} $NaNO_3$ from −0.6 to 0.6 V, and the typical results measured at 1.5 mA·cm^{-2} are shown in Fig. 9. The curve of PANI P3 displays a sharp change in electrode potential during charging and discharging processes when the measured potentials are more negative than approximately 0 V, indicating the absence of faradic reaction in this potential range. After the incorporation of MoO_x into the film, the responses during the anodic charging and cathodic discharging processes are nearly symmetric, demonstrating that the potential window of the film to display pseudocapacitive property extends negatively. The average specific capacitance of the films can be estimated from Eq. 1 [23]:

$$C = i \cdot t / \Delta E \cdot W \quad (1)$$

Table 1 Characteristic FTIR frequencies of PANI–MoO_x C3 and PANI P3

Wavenumber/cm^{-1}		Band characteristics
PANI–MoO_x C3	PANI P3	
1,633.5	1,634.2	Nitrogen quinone rings
1,579.8	1,571.2	Nitrogen benzoid rings
1,385.4	1,384.1	NO_3^- doped in films
1,130.8	1,135.2	Characteristic bands of protonated PANI
961.8		MoO_x
801.9		MoO_x

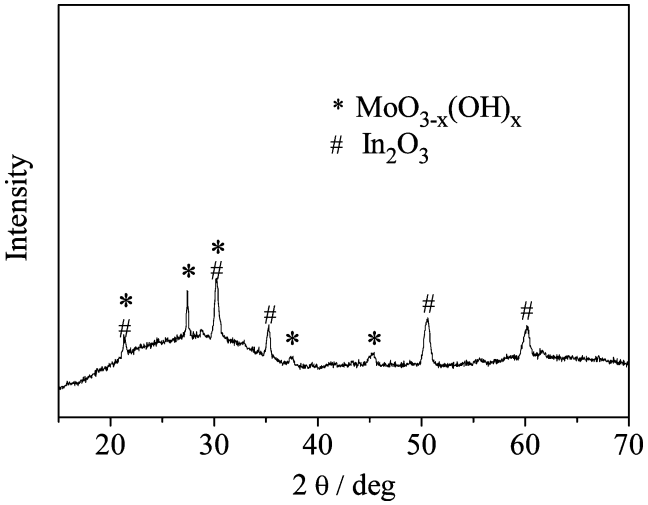

Fig. 11 XRD patterns of PANI–MoO_x C3 electrodeposited on ITO glass

Where i and t are the discharging current density and time, respectively; ΔE and W are the discharging potential window and the amount of the film, respectively. The average specific capacitance obtained on the basis of Eq. 1 is 363.6 and 146.4 F·g^{-1} for PANI–MoO_x C3 and PANI P3, respectively. PANI P3 displays a capacitance of 196.1 F·g^{-1} when the potential window of charge and discharge is limited to 0~0.6 V. The capacitance of the composite film C3 is nearly two times of that of PANI P3 with the potential window enlarged ca. 0.6 V.

Characterization of PANI–MoO_x

Figure 10 is the FTIR spectra of PANI–MoO_x composite C3 (line a) and PANI P3 (line b). The peak locations and

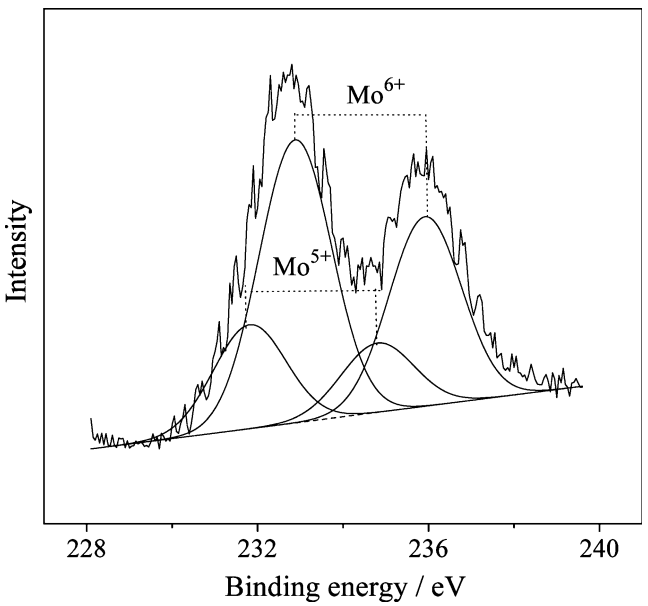

Fig. 12 XPS spectrum of Mo 3d for PANI–MoO_x C3

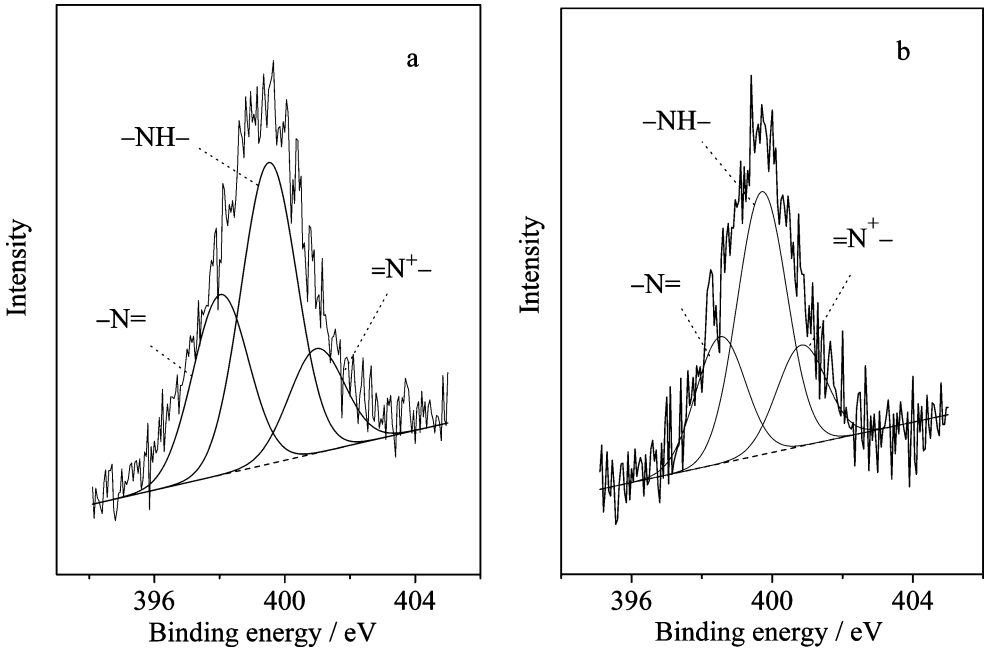

Fig. 13 XPS spectra of N 1s for PANI–MoO_x C3 (**a**) and PANI P3 (**b**)

the corresponding chemical bonds are listed in Table 1. Both of the spectra display the main vibrational bands of PANI at similar wavenumbers. The bands at 1,633.5 and 1,634.2 cm^{-1} are due to nitrogen quinone, while those at 1,579.8 and 1,571.2 cm^{-1} can be assigned to benzoid ring [19, 24]. The characteristic bands of the protonated states of PANI appear at 1,130.8 and 1,135.2 cm^{-1} for PANI–MoO_x C3 and PANI P3, respectively [19, 24]. The peaks at 1,385.4 and 1,384.1 cm^{-1} are due to NO_3^- doped in the films [19, 25]. The peaks for MoO_x appear at 961.8 and 801.9 cm^{-1} on the spectrum of PANI–MoO_x C3 [26].

To determine the composition of the composite film further, XRD measurement is conducted on the film electrodeposited on ITO glass under similar conditions for the deposition of C3. Figure 11 is the XRD patterns of the film. Based on the powder diffraction index cards 47-0186, there are hydrogen molybdenum bronzes in the film in which molybdenum exists in a mixed valence of +5 and +6. There are also signals for In_2O_3 (index card 71-2195) that are due to ITO glass [27].

The surface measurements by XPS are performed, and Fig. 12 shows the XPS core level spectrum of Mo 3d for PANI–MoO_x C3. The broad signals indicate that molybdenum exits in mixed valence states [8]. Deconvolution of the spectrum reveals the doublets for Mo^{6+} at 232.9 and 235.9 eV, and Mo^{5+} at 231.8 and 234.8 eV, respectively. The binding energy and spin-orbit splitting (Δ Mo 3d) are in good agreement with the value reported for mixed-valenced MoO_x by other groups, indicating the existence of MoO_x in the film [11, 28].

The XPS core level spectra of N 1s for PANI–MoO_x C3 (a) and PANI P3 (b) are in Fig. 13. The broad peaks in the spectra indicate that several structures exist in the films. Both of the spectra are reasonable deconvoluted into three Gaussian peaks with the binding energy of 401.3, 399.6, and 398.1 eV for PANI–MoO_x C3 and 400.8, 399.7, and 398.5 eV for PANI P3. As the protonation of PANI occurs preferentially at the imine units [29], the peaks can be ascribed to protonated imine [$=N^+–$], neutral and amine-like nitrogen atoms [–NH–], and neutral and imine-like structue [=N–], respectively [29–32]. The ([=N–] + [$=N^+–$])/[–NH–] ratio for PANI P3 is 0.93, which is very close to the theoretical value of 1 for the 50% intrinsically oxidized emeraldine. The ratio decreases to 0.76 for the PANI–MoO_x C3 film, indicating that some imine species converse into amine species upon composite formation. This may be due to the presence of lower oxidation state molybdenum in the film. The [$=N^+–$]/[=N–] ratio changes from 0.79 to 0.28 after PANI codeposited with MoO_x, showing that PANI is less protonated in the composite film [29]. Some of the protons in the composite may be uptaken by the oxide matrix to form hydrogen molybdenum bronzes through topotactic reaction [30].

Conclusions

The convenient electrochemical synthetic route was limited for organic–inorganic composites based on PANI and oxides due to the incompatible electrodeposition condition for the organic and inorganic moieties. PANI and MoO_x were electrocodeposited in this paper through large-scale dynamic potential scans in slightly acidic to neutral

solutions from aniline and $(NH_4)_6Mo_7O_{24}$. The composition of PANI with MoO_x displayed synergistic effects. The electroreduction of oxoanions on the composite film occurred with enlarged current densities at around 0 V, ca. 0.2 V more positive than that of the similarly prepared MoO_x. The cathodic current around 0 V on the CVs of electrocatalysis is linear with the concentration from 15 to 100 mmol·dm^{-3} for chlorate (current at −0.076 V) and 0.75 to 7.5 mmol·dm^{-3} for bromate (current at −0.007 V), respectively, providing the composite film potential applications in analytical procedures for determining the corresponding oxoanions. The composite film displayed modified pseudocapacitive properties in 1.0 mol·dm^{-3} $NaNO_3$. Upon composition with MoO_x, the pseudocapacitive potential window was at least 0.4 V, negatively extended to −0.6∼0.6 V vs SCE compared to that of PANI-based materials reported so far. While the capacitance was nearly doubled to 363.6 F·g^{-1} from that of PANI when charged–discharged at 1.5 mA·cm^{-2}, even the latter was charged–discharged in a narrow potential window of 0∼0.6 V.

Hydrogen molybdenum bronzes were detected in the XRD diffraction of the composite film. The presence of lower oxidation state molybdenum in the composite film induced the reduction of some imine species to amine, resulting in a low ratio of imine to amine compared to PANI that existed in the form of nearly 50% intrinsically oxidized emeraldine.

Acknowledgment We gratefully acknowledge the financial support from the National Natural Science Foundation of China (project number 50372011), Natural Science Foundation of Liaoning Province, China (project number 20052016), Open Project of Key Laboratory for Supramolecular Structure and Materials (project number KLSSM-200604), and Educational Ministry of China (project number NEU200623).

References

1. Gomez-Romero P (2001) Adv Mater 13:163
2. Stilwell DE, Park S-M (1988) J Electrochem Soc 135:2491
3. Fusalba F, Bélanger D (2000) Electrochim Acta 45:3877
4. Kuwabata S, Idzu T, Martin CR, Yoneyama H (1998) J Electrochem Soc 145:2707
5. Shen PK, Huang HT, Tseung ACC (1992) J Electrochem Soc 139:1840
6. Liu S, Wang B, Liu B, Dong S (2000) Electrochim Acta 45:1683
7. Guerfi A, Paynter RW, Dao LH (1995) J Electrochem Soc 142:3457
8. Laperrière G, Lavoie M-A, Bélanger D (1996) J Electrochem Soc 143:3109
9. Machida K, Enyo M (1990) J Electrochem Soc 137:1169
10. Kosminsky L, Bertotti M (1999) J Electroanal Chem 471:37
11. Wang B, Dong S (1994) J Electroanal Chem 379:207
12. Yao JN, Loo BH, Hashimoto K, Fujishima A (1990) J Electroanal Chem 290:263
13. Takasu Y, Nakamura T, Murakami Y (1998) Chem Lett:1215
14. Sugimoto W, Ohnuma T, Murakami Y, Takasu Y (2001) Electrochem Solid State Lett 4:A145
15. Kerr TA, Wu H, Nazar LF (1996) Chem Mater 8:2005
16. Wang J, Matsubara I, Murayama N, Woosuck S, Izu N (2006) Thin Solid Films 514:329
17. Zhitomirsky I (2002) Adv Colloid Interface Sci 97:279
18. Keita B, Nadjo L, Contant R (1998) J Electroanal Chem 443:168
19. Liu X-X, Zhang L, Li Y-B, Bian L-J, Su Z, Zhang L-J (2005) J Mater Sci 40:4511
20. Genies EM, Boyle A, Lapkowski M, Tsintavis C (1990) Synth Met 36:139
21. Huang W-S, Humphrey BD, MacDiarmid AG (1986) J Chem Soc Faraday Trans 1(82):2385
22. Zou Y-K, He B-L, Zhou W-J, Huang J, Li X-H, Wu B, Li H-L (2004) Electrochim Acta 49:257
23. Musiani M (2000) Electrochim Acta 45:3397
24. Kulkarni MV, Viswanath AK, Marimuthu R, Seth T (2004) Polym Eng Sci 44:1676
25. Mu S, Kan J (1998) Synth Met 98:51
26. He T, Yao J (2003) J Photochem Photobio C Photochem Rev 4:125
27. Salehi A (1998) Thin Solid Films 324:214
28. Fleisch TH, Mains GJ (1982) J Chem Phys 76:780
29. Kang ET, Neoh KG, Tan KL (1998) Prog Polym Sci 23:277
30. Schoellhorn R, Kuhlmann R (1976) Mater Res Bull 11:83
31. Chen Y, Kang ET, Neoh KG (2002) Appl Surf Sci 185:267
32. Park J-E, Park S-G, Koukitu A, Hatozaki O, Oyama N (2004) Synth Met 141:265